

# Spectral-induced polarization characteristics of rock types from the skarn deposit in Gagok Mine, Taebaeksan Basin, South Korea

S. W. Shin · S. G. Park · D. B. Shin

Received: 2 June 2014 / Accepted: 24 December 2014 / Published online: 3 January 2015  
© Springer-Verlag Berlin Heidelberg 2015

**Abstract** Spectral-induced polarization (SIP), which measures the responses to alternative current of multi-frequencies below 1 kHz, is an excellent technique for exploring the economic minerals in the ore deposits. However, the studies on the SIP characteristics of rocks from ore deposits have rarely been conducted due to the decline of mining activities. For effective exploration, the SIP responses of in situ rocks should be recognized first. Therefore, this study was conducted to understand the characteristics of the SIP responses depending on the rock type using the laboratory measurements. Rock samples were obtained from both host rocks and skarn rocks in the Gagok Mine which is a typical skarn deposit in South Korea. The responses of the host rocks, which include dielectric minerals, were found to depend on the induced polarization (IP) effect of the compact layer. In contrast, the responses of the skarn rocks, which were mixtures of dielectric and metallic minerals, depended on the IP effect of the diffuse layer. This study clearly demonstrates that SIP responses are determined by the electrochemical characteristics of the composing minerals.

**Keywords** SIP · Skarn deposit · Rock physical property · Double layer · Chargeability

## Introduction

Over the past decade, the prices of economic minerals have dramatically increased worldwide due to imbalances in supply and demand. Recently, many mineral prospectors have made concerted efforts to discover new reserves. A variety of economic and uncertain risks exist in the mineral exploration business (Singer and Kouda 1999). To reduce these risks, geophysical exploration, which efficiently investigates a huge area, is frequently conducted (Oldenburg and Pratt 2007). For the last 50 years, the induced polarization (IP) has been known as the best geophysical exploration method for investigating certain minerals, such as sulfide metallic minerals, graphite, and alluvial clay (Seigel et al. 2007).

However, the electromagnetic-coupling problem, which is caused in the earliest time domain IP, has been recognized (Hall of 1974; Hohmann et al. 1970). To counter this problem, various methods were suggested, and it is known that Spectral-induced polarization (SIP) based on impedance spectroscopy is the best method (Zonge and Wynn 1975). The SIP has been applied mineral exploration (Pelton et al. 1978; Vanhala and Peltoniemi 1992) as well as in a variety of environmental investigations (Jougnot et al. 2010; Kemna et al. 2004; Revil and Florsch 2010; Vanhala and Soininen 1995; Vanhala et al. 1992; Weller and Börner 1996; Zhdanov 2008). In addition, research on SIP inversions for numerical interpretation has been conducted (Ghorbani et al. 2007; Loke et al. 2006; Routh et al. 1998).

For more effective SIP exploration, the characteristics of SIP responses according to rock type should be defined

---

S. W. Shin · S. G. Park (✉)  
Exploration Geophysics and Mining Engineering Department,  
Korea Institute of Geoscience and Mineral Resources, Gajeong-  
dong 30, Daejeon, Yuseong-Gu 305-350, South Korea  
e-mail: samgyu@kigam.re.kr

S. W. Shin  
e-mail: sw.shin@kongju.ac.kr

S. W. Shin · D. B. Shin  
Department of Geoenvironmental Sciences, Kongju National  
University, Shinkwan-dong 182, Kongju 314-701, South Korea  
e-mail: shin@kongju.ac.kr

(Bishop and Emerson 1999; Collett and Katsube 1973; Emerson 1986; McDowell et al. 2002). However, these characteristics have rarely been studied since the mining industry started to decline in the early 1980s due to the copper price crash (Matthews and Zonge 2003). Therefore, this paper is concentrated on identifying these characteristics using the laboratory measurement of the rocks in the Gagok Mine.

### Geologic setting

The Gagok Mine, which lies in a skarn deposit, is located in a northeastern district of South Korea. The basement rock is Proterozoic Hongjaesa granite that is covered by Cambrian–Ordovician sedimentary formations. The formations of the Choson supergroup consist of the Myobong, Pungchon, Hawjeol, and Dongjeom formations (Fig. 1). The Myobong and Pungchon formations include the bulk of limestone and were intruded by Late Cretaceous quartz monzonite porphyry (Yun 1979).

The orebodies of the Gagok Mine were formed by thermal mineralization induced by the skarn. The mine contains three orebodies: Seongok, Wolgok, and Kumgok. The orebodies included a variety of sulfide minerals, such as sphalerite, galena, chalcopyrite, and pyrrhotite. Ores of

measuring 597,351 MT were produced during 1971–1978 and consisted of Zn 3.93 %, Pb 0.21 %, and Cu 0.11 % (Yun and Einaudi 1982).

### Petrography

Rock samples were obtained from drilling cores and outcrop rocks in the Gagok Mine and were divided into host rocks (limestone, porphyry, and slate) and skarn rocks (skarn and ore). The limestone samples were mud-supported and included massive calcite (Fig. 2a). In addition, the roundness and sorting of the grains were poor (Fig. 2b). The porphyry samples had medium-sized grains from 1 to 2 mm (Fig. 2c) and consisted of quartz, orthoclase, and albite (Fig. 2d). The slate samples were laminated (Fig. 2e) and consisted of biotite, muscovite, and quartz, and their grains were silt-sized (Fig. 2f).

Although the skarn samples were primarily green skarn minerals (Fig. 2g), there were few sulfide minerals, such as sphalerite and pyrrhotite (Fig. 2h). The sulfide minerals in the ore samples were relatively abundant compared to the skarn samples (Fig. 2i, j). Therefore, the host rocks represented the bulk of dielectric minerals, while there were both dielectric and conductive minerals in the skarn rocks.

**Fig. 1** Geological map of Gagok mine area (after Yun and Einaudi 1982)

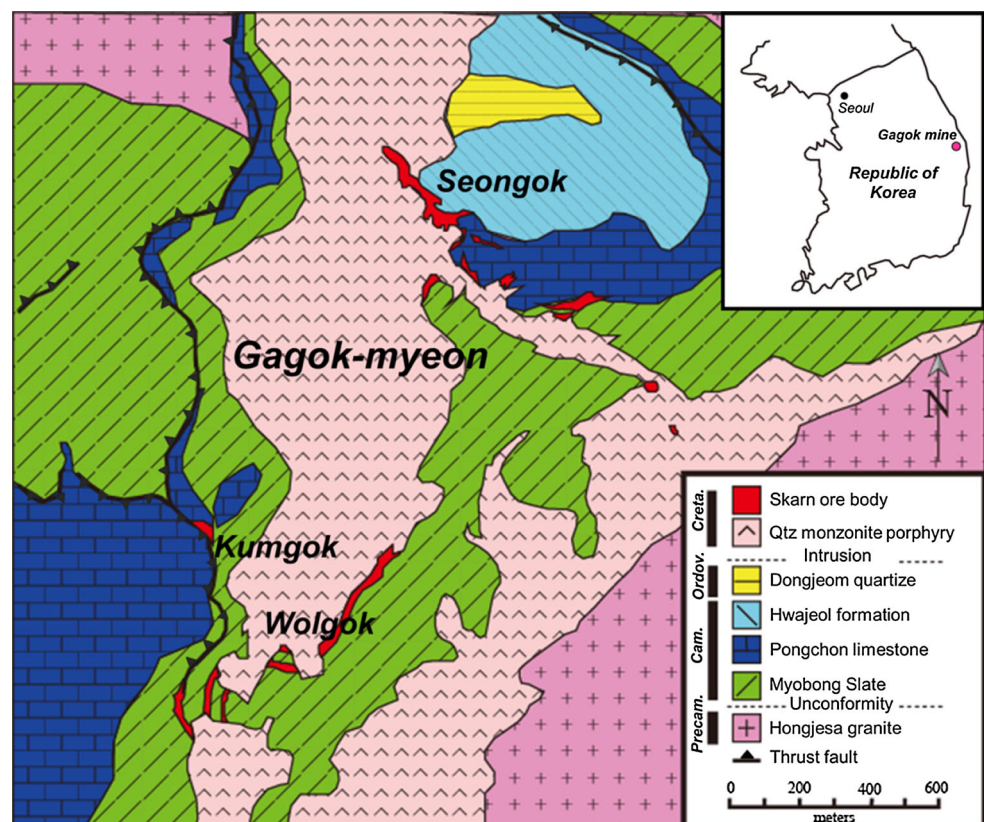
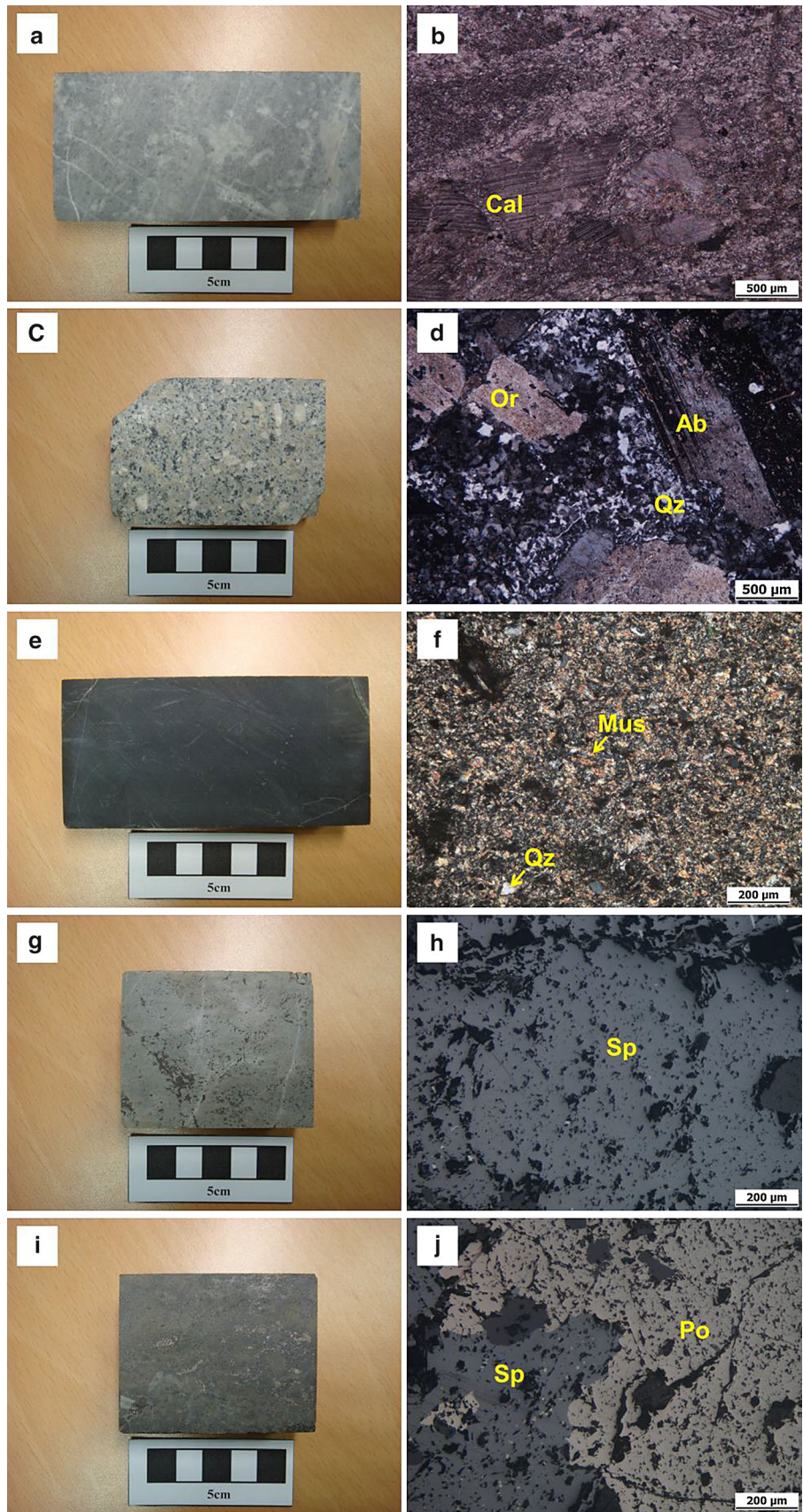




**Fig. 2** Images of rock slab and photomicrograph of each sample (**a, b** limestone3, **c, d** quartz monzonite porphyry1, **e, f** slate3, **g, h** skarn1, **i, j** ore1)



## Laboratory measurement

### Measurement system

The measurement system consisted of a transmitter, two set of electrodes, and a sample holder. The transmitter (LDT-10B, Zonge Co.) is a device that transmits electrical power in the range of  $10^{-3}$  to 10 mA using a constant-current system. The receiver (GDP-32II, Zonge Co.) is an instrument that acquires data as well as controls the waveform of the source. DC is converted to AC within this unit. The equipment was designed to obtain measurements in the frequency range between  $10^{-2}$  and  $10^3$  Hz.

The four-electrode method suggested by Park and Matsui (1998) was used to determine the stable electrical properties of the rock samples. The electrode and rock sample were held in close contact by two screws (on different sides) in the acrylic sample holder.

### Measurement method

When measuring, it is important to constantly keep the electrical density in the sample for accurate data acquisition. The samples were made in cylindrical so that Gauss's symmetry was maintained. The water saturation of the samples complied with the rock standard testing method using a vacuum pump (Bieniawski and Bernede 1979). Brine water was used (0.001 M NaCl) with electrical conductivity similar to that of groundwater.

After saturation, a sample was pulled from the container, and the surface moisture of the samples was wiped using a wet towel. The sample and the electrodes, whose filter paper was soaked with brine (0.01 M NaCl) to reduce the contact resistance, were installed in the measurement holder. The water was poured into the bottom of the measurement holder, and the cover was put on to prevent evaporation from the sample surface.

The sample was measured when completing the installation. The lowest measurement frequency, which takes the longest time, was limited to 0.125 Hz because the SIP data quality is dependent on measurement time.

## Equivalent circuit analysis

The phase and impedance of the polarized rocks change according to the measurement frequency. The electrical double layer (EDL) caused variations, which are electrochemical reactions at the interface between the mineral and solution. The variation of the impedance at a frequency using the complex function is expressed as Eq. 1 (Macdonald and Johnson 2005).

$$z = R(\omega) - jX(\omega). \quad (1)$$

where  $Z$  is the measured impedance,  $R(\omega)$  is the resistive component,  $X(\omega)$  is the capacitance component, and  $j = \sqrt{-1}$ .

The real impedance as a pure resistive component is determined by the electrical conductivity of rocks to direct current. The imaginary impedance caused by the EDL is dependent on the electrical capacitance of the EDL (Macdonald and Johnson 2005). The EDL is divided into a compact layer and a diffuse layer. The compact layer is formed by a non-faradic current at high frequencies. The diffuse layer is formed by a faradic current at low frequencies (Barreto and Dias 2013; Macdonald and Johnson 2005).

The complex impedance of a polarized rock characterizes an equivalent circuit model (Larsson 2009; Macdonald and Johnson 2005). The SIP interpretation technique based on the circuit model is an equivalent circuit analysis. The real impedance characterizes a resistance and the imaginary characterizes impedance capacitance components, such as capacitor, Warburg impedance, and constant phase element. In order to interpret the SIP data of rocks, a variety of the equivalent circuit has been proposed (Dias 2000).

For this study, Dias' circuit model (Fig. 3) was applied because it sufficiently describes the EDL structure (Dias 1972). Z-view (Solatron Co.) program was used to analyze the SIP data, and iterative method was executed to obtain the optimized solution.

The SIP parameters are expressed by the impedance equation described in Eq. 2. Equation 2 is approximated by Eq. 3, whose two parts are classified into the compact layer and the diffuse layer (Barreto and Dias 2013). Using these equations, the SIP parameters were calculated.

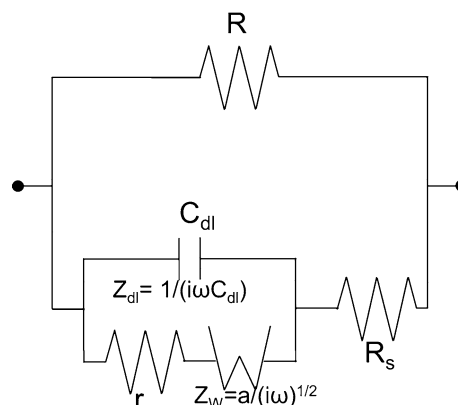
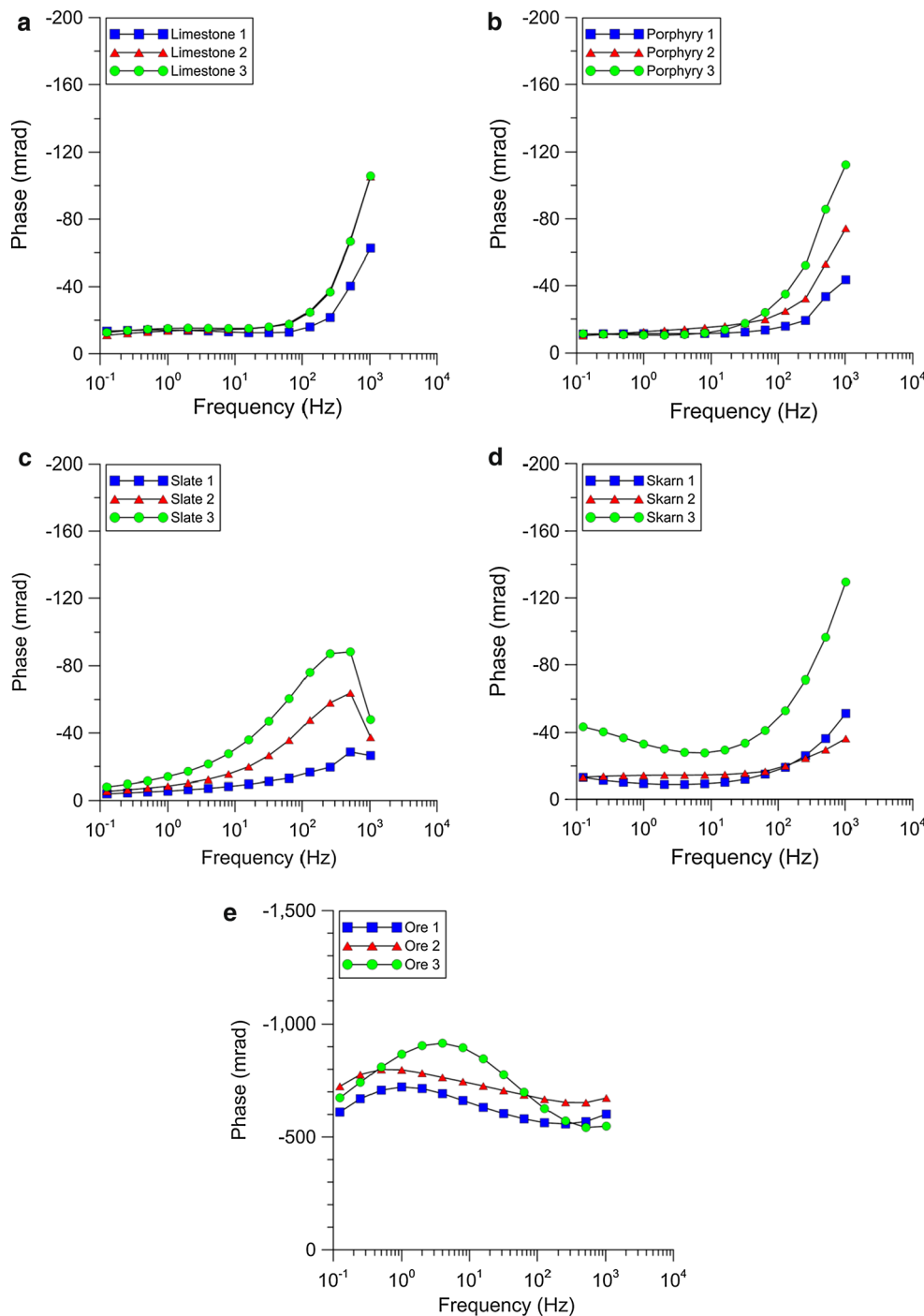


**Fig. 3** Schematic equivalent circuit diagram of Dias model (after Dias 1972)

**Fig. 4** Phase spectra of the rock samples according to rock types



$$\frac{Z^* - Z_\infty}{Z_0} = \frac{m}{1 + i\omega\tau'(1 + \mu^{-1})} \tag{2}$$

$$\frac{Z^* - Z}{Z_0} \cong \frac{m_d}{1 + (i\omega\tau_d)^{1/2}} + \frac{m_c}{1 + i\omega\tau_c} \tag{3}$$

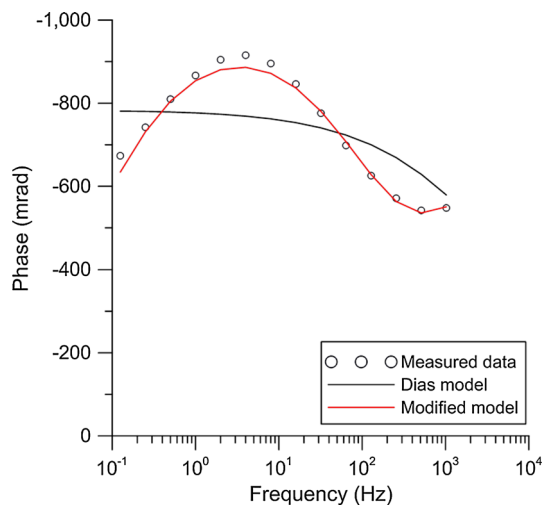
here,  $Z^*$  is the impedance at measurement frequency,  $Z_\infty$  is the impedance at infinity frequency,  $Z_0$  is the impedance at 0 Hz, and  $m$  is the chargeability. The chargeability is

defined as  $m = R/(R + R_S) = m_c + m_d$ , where  $m_c$  is the chargeability of the compact layer calculated as  $m_c = m\tau_c/\tau'$ ,  $m_d$  is the chargeability of the diffuse layer calculated as  $m_d = m\tau_c/\tau$ ,  $\tau$  is the relaxation time calculated as  $\tau = rC_{dl}$ :  $\tau' = (R + R_S) C_{dl}$  and  $\tau'' = (a C_{dl})^2$ ,  $\tau_c$  is the relaxation time of the compact layer calculated as  $\tau_c = \tau\tau' / (\tau + \tau')$ ,  $\tau_d$  is the relaxation time for the diffuse layer calculated as  $\tau_d = [(\tau + \tau')/\tau]^2 \eta^{-2}$ ,  $\eta$  is the



**Table 1** SIP properties computed by analyzed parameters

Sample	$Z_0$ (ohm m)	$m$	$m_w$	$m_D$	NRMSE (%)
Limestone1	7,282	0.2423	0.0640	0.1783	0.6682
Limestone2	9,483	0.3097	0.0555	0.2542	0.8363
Limestone3	9,603	0.3220	0.0521	0.2699	0.9446
Porphyry1	2,754	0.1478	0.0584	0.0893	0.6981
Porphyry2	4,873	0.2447	0.0747	0.1699	0.7174
Porphyry3	12,585	0.2439	0.0563	0.1876	2.6526
Slate1	4,244	0.0854	0.0370	0.0484	0.5169
Slate2	12,194	0.1521	0.0463	0.1059	1.2609
Slate 3	22,452	0.2440	0.1064	0.1377	1.1223
Skarn1	1,447	0.1023	0.0673	0.0350	0.1048
Skarn2	6,745	0.1509	0.0929	0.0580	0.4474
Skarn3	3,033	0.3458	0.1654	0.1804	0.1335
Ore1	196	1.0000	0.9954	0.0046	1.5706
Ore2	284	1.0000	0.9990	0.0009	1.2592
Ore3	144	1.0000	0.9957	0.0042	5.4458

**Fig. 5** Fitting curves using the Dias model and modified model from the result of the Ore3

electrochemical parameter calculated as  $\eta = a/r$ , and  $\mu = i\omega\tau + (i\omega\tau')^{1/2}$ .

## Results and discussion

A graph of the phase spectra was made from the measurement results according to rock type. The phase of host rocks was far smaller at low frequencies below  $10^2$  Hz than at high frequencies (Fig. 4a–c). On the other hand, the phase of the skarn rocks was relatively bigger compared to the phase of the host rocks (Fig. 4d, e). Even the phase of

the ores at low frequencies was bigger than at high frequencies. The phase spectra of the host rocks are considered to correspond with the dielectric phase spectra. However, the phase spectra of the skarn rocks are different. The difference is attributed to the effect of the electrode polarization caused by the sulfide minerals.

The analysis results are summarized as Table 1. The normalized root mean square error (NRMSE) is used to indicate the analysis error (Niranjan 2004). The maximum NRMSE of ores was 13.9233 % when analyzing. Because the value was too big, the Warburg impedance is replaced by the CPE. The NRMSE was dramatically decreased to 5.4468 %, and the analysis result was well fitted (Fig. 5). Therefore, the modification is considered to be effective because the CPE is relatively more useful for analysis of the anomalous SIP response compared to other capacitive components (Katz and Willner 2003).

The resistivity values of host rocks were relatively higher compared to the skarn rocks. The chargeability values of the host rocks were directly proportional to the resistivity value. The chargeability values of the compact layer were higher than the chargeability of the diffuse layer. On the other hand, the chargeability values of the compact layer of the skarn rocks were lower. The chargeability values of the diffuse layer are dominant in the case of the ores (Table 1). The proportion between chargeability and resistivity of the host rocks is explained by the polarization characteristics of the complex dielectric constant (Knight and Nur 1987). The chargeability of the diffuse layer of the skarn rocks is considered to be influenced by the electrode polarization, which is caused by the sulfide minerals (Dias 2000).

## Conclusions

This study was conducted to identify the SIP characteristics according to rock type in the Gagok Mine. The conclusions of this study are given as follows:

- The chargeability of the host rocks is directly proportional to the resistivity, and it is larger than that of the diffuse layer. This is in accordance with the electrochemical characteristics between the general dielectric material and the solution because the host rocks consist of dielectric minerals, such as silicate and carbonate minerals.
- There is no relationship between the chargeability and resistivity of the skarn rocks. In addition, the chargeability of the diffuse layer is greater than that of the compact layer. These observations are considered to be the effect of electrode polarization caused by the sulfide minerals.

- The SIP characteristics of rocks in the Gagok Mine are dependent on the mineral composition. The dielectric minerals are influenced by the IP effect of the compact layer, and the sulfide minerals are affected by the IP effect of the diffuse layer.

**Acknowledgments** This research was supported by the Basic Research Project of the Korea Institute of Geoscience and Mineral Resources (KIGAM) funded by the Ministry of Knowledge Economy of Korea and also an Energy Efficiency and Resources of the Korea Institute of Energy Technology and Planning (KETEP) grant funded by the Korea Government Ministry of Trade, Industry and Energy (MOTIE) (20142510101750).

## References

- Barreto A, Dias C (2013) Complex resistivity decomposition of the Dias's model in partition fractions applied to electrolyte salinity, clay content and hydraulic permeability determination. In: 13th International Congress of the Brazilian Geophysical Society; EXPOGEF, Rio de Janeiro, Brazil, 26–29 August 2013, pp 1095–1104. doi:10.1190/sbgf2013-226
- Bieniawski ZT, Bernede MJ (1979) Suggested methods for determining the uniaxial compressive strength and deformability of rock materials: Part 1. Suggested method for determining deformability of rock materials in uniaxial compression. *Int J Rock Mech Min Sci Geomech Abstr* 16:138–140. doi:10.1016/0148-9062(79)91451-7
- Bishop JR, Emerson DW (1999) Geophysical properties of zinc-bearing deposits. *Aust J Earth Sci* 46:311–328. doi:10.1046/j.1440-0952.1999.00706.x
- Collett LS, Katsube TJ (1973) Electrical parameters of rocks in developing geophysical techniques. *Geophysics* 38:76–91. doi:10.1190/1.1440336
- Dias CA (1972) Analytical model for a polarizable medium at radio and lower frequencies. *J Geophys Res* 77:4945–4956. doi:10.1029/JB077i026p04945
- Dias CA (2000) Developments in a model to describe low-frequency electrical polarization of rocks. *Geophysics* 65:437–451. doi:10.1190/1.1444738
- Emerson DW (1986) Physical properties of skarns. *Explor Geophys* 17:201–212. doi:10.1071/EG986201
- Ghorbani A, Camerlynck C, Florsch N, Cosenza P, Revil A (2007) Bayesian inference of the cole-cole parameters from time- and frequency-domain induced polarization. *Geophys Prospect* 55:589–605. doi:10.1111/j.1365-2478.2007.00627.x
- Hallof P (1974) The IP phase measurement and inductive coupling. *Geophysics* 39:650–665. doi:10.1190/1.1440455
- Hohmann GW, Kintzinger PR, Vanvoorhis GD, Ward SH (1970) Evaluation of the measurement of induced electrical polarization with an inductive system. *Geophysics* 35:901–915. doi:10.1190/1.1440136
- Jougnot D, Ghorbani A, Revil A, Leroy P, Cosenza P (2010) Spectral-induced polarization of partially saturated clay-rocks: a mechanistic approach. *Geophys J Int* 180:210–224. doi:10.1111/j.1365-246X.2009.04426.x
- Katz E, Willner I (2003) Probing biomolecular interactions at conductive and semiconductive surfaces by impedance spectroscopy: routes to impedimetric immunosensors, DNA-sensors, and enzyme biosensors. *Electroanalysis* 15:913–947. doi:10.1002/elan.200390114
- Kemna A, Binley A, Slater L (2004) Crosshole IP imaging for engineering and environmental applications. *Geophysics* 69:97–107. doi:10.1190/1.1649379
- Knight RJ, Nur A (1987) The dielectric constant of sandstones, 60 kHz to 4 MHz. *Geophysics* 52:644–654. doi:10.1190/1.1442332
- Larsson O (2009) Polarization characteristics in polyelectrolyte thin film capacitors: targeting field-effect transistors and sensors. Linköping University Electronic Press
- Loke MH, Chambers JE, Ogilvy RD (2006) Inversion of 2D Spectral-induced polarization imaging data. *Geophys Prospect* 54:287–301. doi:10.1111/j.1365-2478.2006.00537.x
- Macdonald JR, Johnson WB (2005) Fundamentals of impedance spectroscopy. In: *Impedance spectroscopy*. John Wiley & Sons, Inc., Washington DC, pp 1–26. doi:10.1002/0471716243.ch1
- Matthews P, Zonge KL (2003) 50 years state of the art in ip and complex resistivity KEGS 50th anniversary symposium mining and environmental geophysics—past, present and future Saturday, March 8, 2003, Toronto, Ontario pp 1–18
- McDowell PW, Barker RD, Butcher AP, Culshaw M, Jackosn PD, McCann DM, Arthur JCR (2002) *Geophysics in civil engineering* Geological Society, London, vol 19. Engineering Geology Special Publications, London, pp 19–22. doi:10.1144/gsl.eng.2002.019.01.01
- Niranjan U (2004) Simultaneous storage of medical images in the spatial and frequency domain: a comparative study. *Biomed eng online* 3:17
- Oldenburg DW, Pratt DA (2007) Geophysical inversion for mineral exploration: a decade of progress in theory and practice B Milkereit (Ed). In: *Proceedings of exploration 07: fifth decennial international conference on mineral exploration* pp 66–95
- Park S, Matsui T (1998) Basic study on resistivity of rocks; Ganseki hiteiko ni kansuru kisoteki kenkyu. *Butsuri Tansa (Geophys Explor)* 51(3):201–209 PBD: Jun 1998
- Pelton W, Ward S, Hallof P, Sill W, Nelson P (1978) Mineral discrimination and removal of inductive coupling with multifrequency. *Geophysics* 43:588–609. doi:10.1190/1.1440839
- Revil A, Florsch N (2010) Determination of permeability from Spectral-induced polarization in granular media. *Geophys J Int* 181:1480–1498. doi:10.1111/j.1365-246X.2010.04573.x
- Routh P, Oldenburg D, Li Y (1998) Regularized inversion of spectral IP parameters from complex resistivity data. In: *SEG technical program expanded abstracts 1998*. pp 810–813. doi:10.1190/1.1820608
- Seigel H, Nabighian M, Parasnis D, Vozoff K (2007) The early history of the induced polarization method. *Lead Edge* 26:312–321. doi:10.1190/1.2715054
- Singer D, Kouda R (1999) Examining risk in mineral exploration. *Nat Resour Res* 8:111–122. doi:10.1023/a:1021838618750
- Vanhala H, Peltoniemi M (1992) Spectral IP studies of Finnish ore prospects. *Geophysics* 57:1545–1555. doi:10.1190/1.1443222
- Vanhala H, Soininen H (1995) Laboratory technique for measurement of Spectral-induced polarization response of soil samples I. *Geophys Prospect* 43:655–676. doi:10.1111/j.1365-2478.1995.tb00273.x
- Vanhala H, Soininen H, Kukkonen I (1992) Detecting organic chemical contaminants by spectral-induced polarization method in glacial till environment. *Geophysics* 57:1014–1017. doi:10.1190/1.1443312
- Weller A, Börner FD (1996) Measurements of Spectral-induced polarization for environmental purposes. *Environ Geol* 27:329–334. doi:10.1007/bf00766702
- Yun S (1979) Structural and compositional characteristics of skarn zinc-lead deposits in the Yeonhwa-Ulchin mining district, southeastern Taebaegsan region, Korea: part II. *Yeonhwa II mine J Korean Inst Min Geol* 12:147–176
- Yun S, Einaudi MT (1982) Zinc-lead skarns of the Yeonhwa-Ulchin district. *South Korea Econ Geol* 77:1013–1032. doi:10.2113/gsecongeo.77.4.1013
- Zhdanov M (2008) Generalized effective-medium theory of induced polarization. *Geophysics* 73:F197–F211. doi:10.1190/1.2973462
- Zonge K, Wynn J (1975) Recent advances and applications in complex resistivity measurements. *Geophysics* 40:851–864. doi:10.1190/1.1440572